

## POSSIBILITIES OF Fe-RICH PHASES ELIMINATION WITH USING HEAT TREATMENT IN SECONDARY Al-Si-Cu CAST ALLOY

Received – Primljeno: 2014-01-30

Accepted – Prihvaćeno: 2014-07-15

Original Scientific Paper – Izvorni znanstveni rad

The mechanical properties of Al-Si-Cu cast alloy are strongly dependent upon the morphologies, type and distribution of the second phases. The skeleton like -  $Al_{15}(FeMn)_3Si_2$  and needles -  $Al_5FeSi$  phases were observed in experimental material AlSi9Cu3. The Fe-rich phases morphology was affected with applying two types of heat treatment; T4 and T6, which caused positive changes of mechanical properties especially ultimate tensile strength; gives that for as cast state was  $R_m = 211$  MPa, than at optimum T4 (515 °C/ 4 hours) was  $R_m = 273$  MPa and at optimum T6 (515 °C/ 4 hours with artificial aging 170 °C/ 16 hours) was  $R_m = 311$  MPa.

*Key words:* Al - Si - Cu cast alloy, heat treatment, mechanical properties, microstructure, Fe-rich phases

### INTRODUCTION

Aluminium alloys are ideal replace materials in the car thanks to good formability, good corrosion and wear resistance, high strength stiffness to weight ratio, low density and thermal expansion, and recycling possibilities [1-3].

Due to the increasing production of secondary (recycled) aluminium cast alloys their strict microstructures control is necessary. The additions Cu, Fe, Mn, Mg and Zn produce a lot of intermetallic phases during solidification in Al-Si-Cu alloys [2,4,5-8]. For die casting, Fe is added to increase hot tear resistance and to reduce die sticking. Taylor [8] reported that as Fe levels increase, the ductility of Al-Si based alloys decreases. This is usually accompanied by a decrease in ultimate tensile strength. The detrimental effect of iron on ductility is due to two main reasons [9-13]: (1) the size and number density of iron-containing intermetallic phases (particularly  $\beta$ -phase -  $Al_5FeSi$ ) increases with iron content. (2) as iron level increases, porosity increases, and this defect also has an impact on ductility. In Al-Si-Cu type alloys, however, Fe showed to have the most detrimental effect on material properties of all of the common impurities. These parameters can be affected with chemical treatment, solid solution hardening and precipitation hardening [14-18].

The alloy and its heat treatment presented in this work is part of a larger project and the same microstructural and mechanical property details of which have already been published [18, 19].

### EXPERIMENTAL WORK

As an experimental material was used secondary hypoeutectic AlSi9Cu3 alloy, that contains 9,4 % Si, 2,4 % Cu, 0,9 % Fe, 0,28 % Mg, 0,24 % Mn, 1,0 % Zn, 0,03 % Sn, 0,09 % Pb, 0,04 % Ti, 0,05 % Ni, 0,04 % Cr.

Structure hypoeutectic AlSi9Cu3 cast alloy consists of dendrites  $\alpha$ -phase (light grey), eutectic ( $\alpha$ -phase + eutectic Si) and intermetallic Fe- and Cu-rich phases [18,19] (Figure 1). The melt was not modified or grain refined and so eutectic Si particles are in platelets form, which are needles on scratch pattern (Figure 1-b).

AlSi9Cu3 cast alloy has lower corrosion resistance and is suitable for high temperature applications (dy-

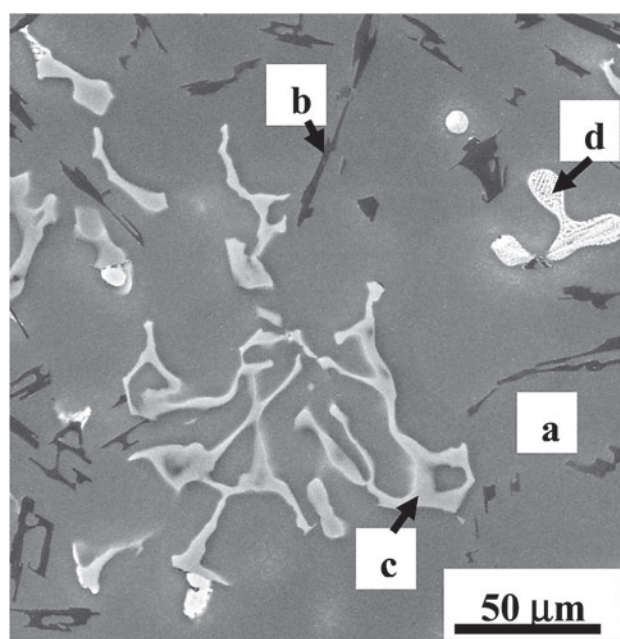


**Figure 1** AlSi9Cu3 cast alloy microstructure in untreated (as-cast) state: (a)  $\alpha$ -phase; (b) eutectic Si; (c) Fe-rich phases; (d) Cu-rich phases; etch. 0,5 % HF, SEM

dynamic exposed casts, where are not so big requirements on mechanical properties) - it means to max. 250 °C. The AlSi9Cu3 alloy has these technological properties: tensile strength (240 - 310 MPa), offset 0,2 % yield stress (140 - 240 MPa), however the low ductility limits (0,5 - 3 %) and hardness HB 80 - 120 [18,19].

The microstructures of experimental material was studied using an optical microscope Neophot 32 and SEM observation with EDX analysis using scanning electron microscope VEGA LMU II linked to the energy dispersive X-ray spectroscopy (EDX analyser Brucker Quantax).

Experimental mechanical test samples were heat treated (T4 - hardening, T6 - age-hardening) in order to affect Fe-rich phases morphology. The heat treatment T4 consists of solution treatment at temperature (505, 515 and 525 °C) with different holding time 2, 4, 8, 16 and 32 hours, quenching and natural aging for 24 hours.

Previous studies showed that optimum heat treatment for such experimental material is: solution treatment at 515 °C with 4 hours. Therefore, the heat treatment T6 consists of solution treatment at 515 °C with holding time 4 hours, quenching and artificial aging at different temperatures 130, 150, 170, and 210 °C with different holding time 2, 4, 8, 16 and 32 hours.

After heat treatment were samples subjected for mechanical test (strength tensile) and structure assessments.

## RESULTS AND DISCUSSION

The Fe detrimental effect on ductility is due to its stress-raising potential and poor binding strength with the matrix [20]. Therefore, the ultimate tensile strength was especially measured from all mechanical properties.

The results of ultimate tensile strength after the T4 heat treatment show Figure 2. Significant strengthening occurs after aging at more than 2 hours (7 200s) for all solution treatment temperatures. First aging peak we can see at holding time 4 hours after hardening at 515 and 525 °C. With further increase in solution time more than 4 hours, tensile strength gently decreases as a result of over-aging [18,19]. The strength peak is achieved approximately at 8 hour after 505 °C heat treatment. Highest ultimate tensile strength 273 MPa was observed at temperature 515 °C with holding time 4 hours after

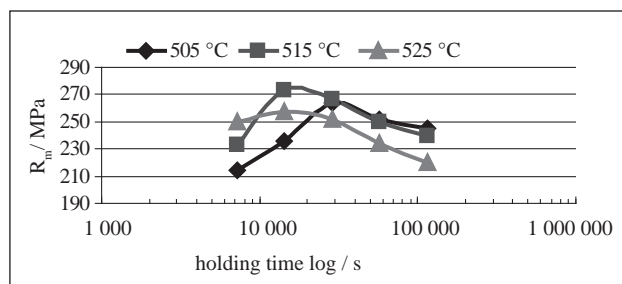


**Figure 2** T4 heat treatment influence on ultimate tensile strength

heat treatment T4 and lowest 211 MPa in as cast state. Hardening at room temperature (T4), although by no means insignificant, is very slow with time.

More rapid and more appreciable hardening occurs at enhanced temperatures - age-hardening T6. The heat treatment T6 is known with double-peak phenomenon. This phenomenon is seeing on curves of ultimate tensile strength of experimental material, too (Figure 3). The first peak was observed after 4 hours for temperature 150 and 170 °C and the second peak after 16 hours. With further increase in solution time more than 16 hours, ultimate tensile strength gently decreases as a result of over-aging.

After age hardening 130 °C was measured only one aging peak. The maximum ultimate tensile strength is achieved at a slow time - 16 hours. At a higher temperature - 210 °C is observed strengthening peak quickly at 8 hours, in compare with used lowest temperature (130 °C).

From these point results, that probably longer holding time of heat treatment at 130 °C is needed for achievement second peak and at 210 °C probably shorter holding time as 2 hour, because at this temperature occurs rapid softening after obtained strengthening peak. Highest ultimate tensile strength 311 MPa was observed for artificial aging 170 °C/ 16 hours after T6 treatment.

The Fe-rich particles can be twice as large as the Si particles, and the cooling rate has a direct impact on the kinetics, quantities and size of Fe-rich intermetallic present in the microstructure [2]. The Fe-rich intermetallic phases group  $\alpha$  (skeleton-like or Chinese script-like phase  $Al_{15}(FeMn)_3Si_2$  - Figure 4) and  $\beta$  ( $Al_3FeSi$  - Figure 5) were observed in experimental secondary AlSi9Cu3 cast alloy. Significant levels of Fe (e.g. > 0,5 %) can change the solidification characteristics of Al-Si alloys by forming pre- and post-eutectic  $Al_3FeSi$ , but when the Fe:Mn rate is 2:1 the formation is limited [9-10]. Experimental material contains less than 0,9 % of Fe and 0,44 % Mn and therefore the intermetallic phase's group  $\beta$  were observed only in a few volumes. Therefore, study is mostly focused on changes of intermetallic phase group  $\alpha$ .

The evolution of Fe-rich phase's group  $\alpha$  during heat treatments T4 and T6 is described in Figure 6. Phase has a compact skeleton-like morphology (Figure 6a) in the as-cast state. Solution treatment and natural aging tends

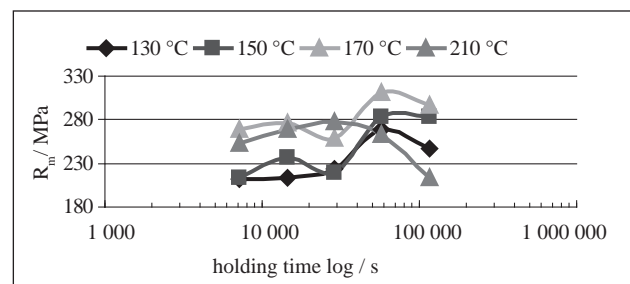


**Figure 3** T6 heat treatment influence on ultimate tensile strength

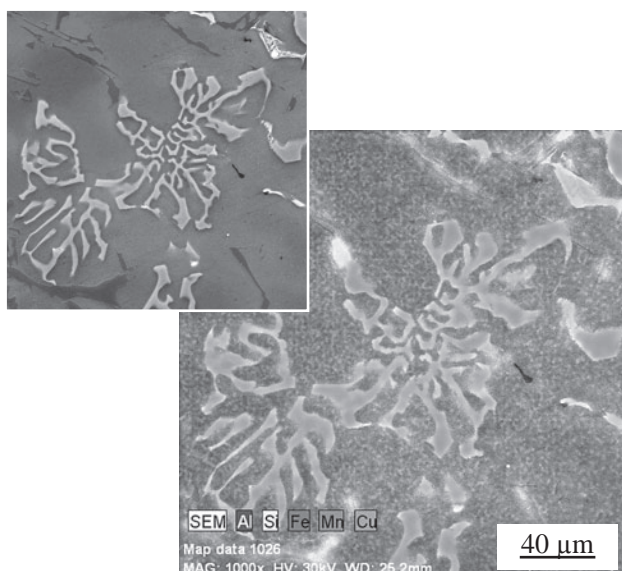


**Figure 4** Morphology of  $\text{Al}_{15}(\text{FeMn})_3\text{Si}_2$ , EDX-mapping, etch. 0,5 % HF, SEM

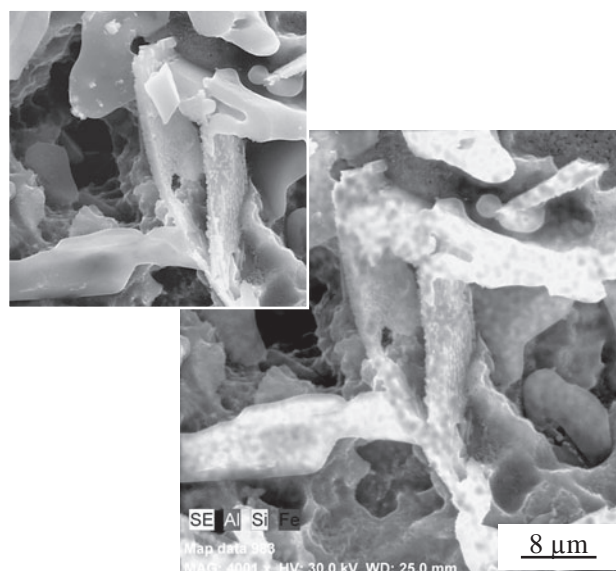


**Figure 5** 3D Morphology of  $\text{Al}_5\text{FeSi}$ , EDX-mapping, deep-etch. HCl, SEM

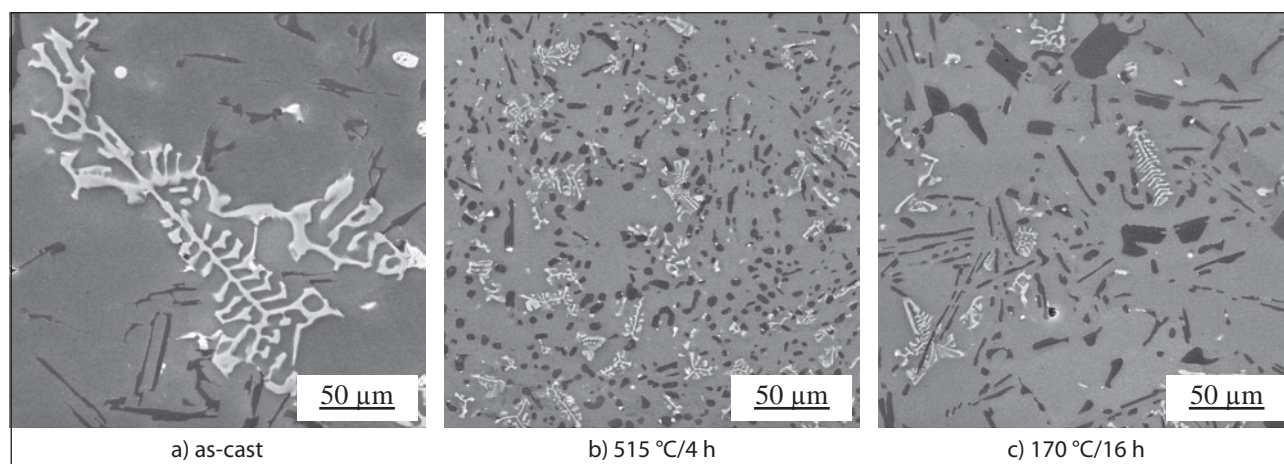


**Figure 6** Changes in morphology of  $\text{Al}_{15}(\text{FeMn})_3\text{Si}_2$ , phases during heat treatments, etch.  $\text{H}_2\text{SO}_4$ , SEM

to fragmentation, segmentation and dissolution of skeleton-like Fe-phases (Figure 6b,c).

Solution treatment at 505 °C tends to fragmentation and at 515 or 525 °C to segmentation of this skeleton-like phase (Figure 6b). The same changes were observed after heat treatment T6, as shown Figure 6c.  $\text{Al}_5\text{FeSi}$  phase is dissolved into very fine needles (difficult to observe). It was established, that the different heat treatment led not only to fragmentation of  $\text{Al}_{15}(\text{MnFe})_3\text{Si}_2$  phase, but also to decrease of area fraction of all Fe-rich phases in  $\text{AlSi9Cu3}$  alloy. Therefore, the quantitative assessment was used.

Quantitative metallography [21] was carried out on Image Analyzer NIS - Elements to quantify Fe-rich phases (average area) morphology changes, and changes in area fraction during treatments. The maximum average area of Fe-rich phases was observed in as-cast samples ( $1128 \mu\text{m}^2$ ). The increasing solution temperature causes changes of Fe-phases average area from  $72 \mu\text{m}^2$  to  $839 \mu\text{m}^2$  in samples T4 heat treated (Figure 7). The average area of Fe-rich phases was higher at 505 °C and lower at 515 and 525 °C. With a prolonged solution

treatment time at 515 °C and 525 °C more than 2 h, the extent of Fe-rich phase's dissolution changed little.

The heat treatment T6 reduces average area of Fe-rich intermetallic phases more than heat treatment T4 (Figure 8). The average area of Fe-rich phases at artificial aging 130 °C up to 210 °C was from  $47 \mu\text{m}^2$  to  $129 \mu\text{m}^2$ . Lowest average area was at temperature 515 °C after T4 heat treatment and at 170 °C after T6 heat treatment.

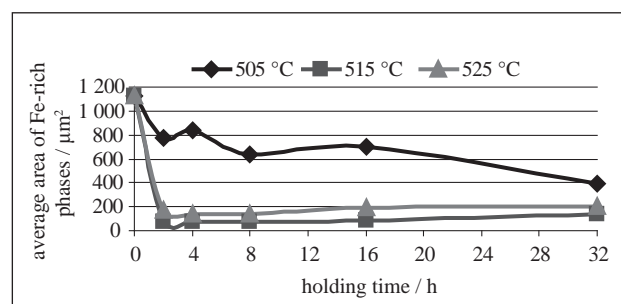


**Figure 7** Changes in average area of  $\text{Al}_{15}(\text{FeMn})_3\text{Si}_2$  phases during heat treatment T4

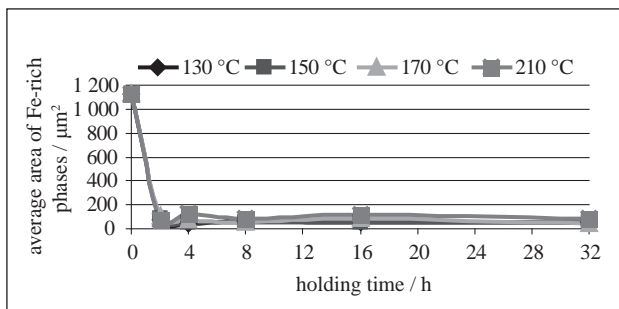


**Figure 8** Changes in average area of  $Al_{15}(FeMn)_3Si_2$  phases during heat treatment T6

## CONCLUSIONS

This experimental work results in:

- The morphology and size of iron phases are dependent on the heat treatment in  $AlSi9Cu3$ .
- After T4 skeleton-like  $Al_{15}(FeMn)_3Si_2$  phases were fragmented and dissolved (average area reduces from 1128 to 72  $\mu m^2$ ).
- The age-hardening (T6) caused great changes of Fe-rich phases too (average area reduces from 1128 to 47  $\mu m^2$ ).
- The Fe rich intermetallic phases in needles form were dissolved into very fine needles. These particles were difficult to observe already at T4 heat treatment.

## Acknowledgements

The authors acknowledge the financial support of the project VEGA No 1/0841/11 and European Union - the Project ITMS: 26110230117.

## REFERENCES

- [1] Castings, Available on line: <http://www.aluminum.org/content/navigationmenu/theindustry/castings/default.htm>

- [2] M. A. Moustafa. *Journal of Materials Processing Technology*, 209 (2009), 605-610.
- [3] M. Matvija et al. *Acta Metallurgica Slovaca*, 18 (2012) 1, 4-12.
- [4] S. Seifeddine. Literature review - Vilmer project. Jönköping University, Sweden, 2007.
- [5] W. Khraisat et al. *Journal Mechanical and Industrial Engineering*, 4 (2010) 3, 372-337.
- [6] X. Fang et al. *Materials science and engineering. A - Structural materials: properties, microstructure and processing*. 445-446 (2007), 65-72.
- [7] L. Lu et al. *Metallurgical and transactions A*, 36A (2005), 819-835J.
- [8] J. A. Taylor. 35th Australian Foundry Institute National Conference, Adelaide, South Australia, 2004, pp. 148-157.
- [9] C. H. Cáceres et al. in *Scripta Materialia*, Vol. 40 (1999) 5, pp. 631-637.
- [10] A. M. Samuel et al. *Journal of Materials Science*, 31 (1996), 5529-5539.
- [11] S. G. Shabestari. *Materials Science and Engineering A*, 383 (2004), 289-298.
- [12] P. Ashtari et al. *Scripta Materialia* Vol. 53 (2005), pp. 937-942.
- [13] E. Sjölander et al. *Journal of Materials Processing Technology*, 210 (2010) 10, 1249-1259.
- [14] M. Tash et al. *Materials Science and Engineering, A* 443 (2007), 185-201.
- [15] M. Abdulwahab. *Australian Journal of Basic and Applied Sciences*, 2 (2008) 4, 839-843.
- [16] H. G. Johansen. *TALAT Lecture 2202 - Basic Level*, (1994), pp. 2-28.
- [17] Solutions for ductile die casting, available on line: <http://foundry-planet.com/fileadmin/redakteur/werbepartner/sag/SolutionsDuctileDieCasting>.
- [18] L. Hurtalová et al. *International Journal of Applied Mechanics and Engineering*, 15 (2010) 2, 355-362.
- [19] E. Tillová et al. *Communications*, 12 (2010) 4, 95-101.
- [20] Ma Z. et al. *Materials Science and Engineering, A* 490 (2008), 36-51.
- [21] A. Vaško et al. *Improvement of Quality Regarding Processes and Materials: Borkowski, S. and Tillova, E., PTM, Warszawa, (2007), pp. 53-58.*

**Note:** The responsible translator for English language is Otakar Bokůvka, Žilina, Slovakia